

A physics-based, deformable soil model for estimating a military vehicle's power/energy requirements

George Bozdech^a, Paul Ayers^{a,*}, Jeff Freeman^b, and Alexander Reid^c

^a Department of Biosystems Engineering and Soil Science, University of Tennessee, 2506 E.J. Chapman Drive, Knoxville, TN 37996, USA

^b Mechanical Simulation Incorporated, 604 Lakeland Crescent, Yorktown, VA 23693

^c U.S. Army Tank Automotive RDEC, 6501 E. 11 Mile Road, MS: ASMSRD-TAR-N #157, Warren, MI 48397

gbozdech@utk.edu ((309) 264 - 5081), pdayers@utk.edu, Jeff.Freeman@mechsim.com, Alexander.A.Reid@us.army.mil

Abstract

A physics-based, deformable soil model was developed for use in the U.S. Army's Tank Automotive Research, Development Engineering Center's (TARDEC) real-time vehicle-motion simulator. The power dissipated from the tires of the U.S. Army's 8-wheeled Stryker vehicle are predicted while the vehicle traverses a Unified Soils Classification System (USCS) CL soil type. The results from the following components of the model are presented: the vertical soil deformation of a single soil element due to the surface loads generated from a Stryker vehicle's tires, the power dissipated by the vehicle while turning due to the lateral bulldozing of the soil, and the power required for a single Stryker tire to longitudinally bulldoze the soil. The predicted bulk density increase of the soil element decreased as the travel speed and the number of passes of the Stryker tires increased. The lateral displacement from the Stryker vehicle's eight tires and the associated power requirement increased as the travel speed increased and the vehicle turning radius decreased. The results from the longitudinal bulldozing model indicated that the power required to overcome the longitudinal bulldozing from a Stryker tire increased as the tire sinkage (rut depth), vehicle travel speed, and the soil's angle of internal friction increased.

Keywords: physics-based, soil model, power, energy, Stryker, military vehicle

1. Introduction

The current Vehicle Terrain Interaction (VTI) model used in real-time, vehicle-motion simulator estimates the motion resistance and power requirements of military vehicles via semi-empirical equations. The equations were developed from test data collected for previous and current U.S. military vehicles operating in coarse-grained and fine-grained soils. However, the current VTI model is more applicable to military vehicles with similar characteristics to the vehicles that were tested. Attributes of current and future military vehicles may differ substantially from the vehicles that were

Report Documentation Page

Form Approved
OMB No. 0704-0188

Public reporting burden for the collection of information is estimated to average 1 hour per response, including the time for reviewing instructions, searching existing data sources, gathering and maintaining the data needed, and completing and reviewing the collection of information. Send comments regarding this burden estimate or any other aspect of this collection of information, including suggestions for reducing this burden, to Washington Headquarters Services, Directorate for Information Operations and Reports, 1215 Jefferson Davis Highway, Suite 1204, Arlington VA 22202-4302. Respondents should be aware that notwithstanding any other provision of law, no person shall be subject to a penalty for failing to comply with a collection of information if it does not display a currently valid OMB control number.

1. REPORT DATE 01 OCT 2012	2. REPORT TYPE Journal Article	3. DATES COVERED 10-05-2012 to 28-09-2012			
4. TITLE AND SUBTITLE A physics-based, deformable soil model for estimating a military vehicle's power energy requirements		5a. CONTRACT NUMBER			
		5b. GRANT NUMBER			
		5c. PROGRAM ELEMENT NUMBER			
6. AUTHOR(S) George Bozdech; Paul Ayers; Jeff Freeman; Alexander Reid		5d. PROJECT NUMBER			
		5e. TASK NUMBER			
		5f. WORK UNIT NUMBER			
7. PERFORMING ORGANIZATION NAME(S) AND ADDRESS(ES) Department of Biosystems Engineering and Soil Science, University of Tennessee, 2506 E.J. Chapman Drive, Knoxville, TN, 37996		8. PERFORMING ORGANIZATION REPORT NUMBER ; #23246			
9. SPONSORING/MONITORING AGENCY NAME(S) AND ADDRESS(ES) U.S. Army TARDEC, 6501 East Eleven Mile Rd, Warren, Mi, 48397-5000		10. SPONSOR/MONITOR'S ACRONYM(S) TARDEC			
		11. SPONSOR/MONITOR'S REPORT NUMBER(S) #23246			
12. DISTRIBUTION/AVAILABILITY STATEMENT Approved for public release; distribution unlimited					
13. SUPPLEMENTARY NOTES					
14. ABSTRACT A physics-based, deformable soil model was developed for use in the U.S. Army's Tank Automotive Research, Development Engineering Center's (TARDEC) real-time vehicle-motion simulator. The power dissipated from the tires of the U.S. Army's 8-wheeled Stryker vehicle are predicted while the vehicle traverses a Unified Soils Classification System (USCS) CL soil type. The results from the following components of the model are presented: the vertical soil deformation of a single soil element due to the surface loads generated from a Stryker vehicle's tires, the power dissipated by the vehicle while turning due to the lateral bulldozing of the soil, and the power required for a single Stryker tire to longitudinally bulldoze the soil. The predicted bulk density increase of the soil element decreased as the travel speed and the number of passes of the Stryker tires increased. The lateral displacement from the Stryker vehicle's eight tires and the associated power requirement increased as the travel speed increased and the vehicle turning radius decreased. The results from the longitudinal bulldozing model indicated that the power required to overcome the longitudinal bulldozing from a Stryker tire increased as the tire sinkage (rut depth), vehicle travel speed, and the soil's angle of internal friction increased.					
15. SUBJECT TERMS physics-based, soil model, power, energy, Stryker, military vehicle					
16. SECURITY CLASSIFICATION OF:			17. LIMITATION OF ABSTRACT Public Release	18. NUMBER OF PAGES 15	19a. NAME OF RESPONSIBLE PERSON
a. REPORT unclassified	b. ABSTRACT unclassified	c. THIS PAGE unclassified			

used to develop the semi-empirical equations. Such attributes as the track/tire geometry, track/tire composition, vehicle weight, and vehicle size of current and future military vehicles may differ substantially, especially considering the increasing use of smaller, Unmanned Ground Vehicles (UGV) for U.S. military operations. There is a need for an updated VTI model that is scalable and independent of vehicle size and weight in order to allow for more accurate estimates of a vehicle's motion resistance and the subsequent power and energy requirements during off-road locomotion. A physics-based, deformable soil model that is applicable to all U.S. military vehicles represents one possible solution for estimating the real-time power and energy required to overcome the motion resistance generated by the tractive elements due to the deformation of the soil. Furthermore, Madsen et al.(2012) indicate that computationally intensive Discrete Element Method (DEM) or Finite Element Method (FEM) approaches for characterizing the soil's response to a vehicle are impractical for use in a real-time, vehicle-motion simulator [1].

2. Objectives

The specific objectives of this study were the following:

1. develop a physics-based, deformable soil model,
2. apply the vertical deformation portion of the model to a single soil element subject to loading from the eight tires of a U.S. Army Stryker vehicle,
3. estimate the lateral displacement and power dissipated due to the lateral bulldozing of the soil by the Stryker vehicle along with the vehicle's maximum possible travel speed during turning, and
4. predict the power dissipated due to the longitudinal bulldozing of a single Stryker tire.

3. Model development

3.1 Vertical soil deformation (sinkage) due to surface forces

3.1.1 Vertical soil stress distribution due to a normal surface load (Boussinesq model)

Since the tire-soil surface contact area and the vehicle normal surface loads are known, the subsurface stress distribution needs to be estimated to predict deformation of the soil. The method for calculating the stress distribution in a semi-infinite, homogeneous, isotropic, elastic medium subject to a vertical point load applied on the surface was first developed by Boussinesq:

$$\sigma_z = \frac{3}{2\pi} \frac{1}{[1+(r/z)^2]^{5/2}} \frac{W}{z^2} \quad (1)$$

Where σ_z is the vertical stress at the depth z , W is the point load, and r is the horizontal distance from the point load to the point in equation [2]. This is shown in Fig. 1.

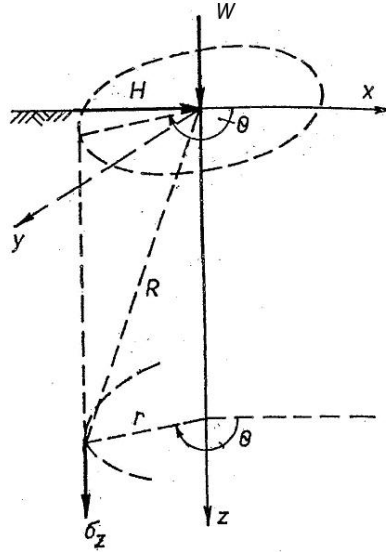


Fig. 1. Subsurface soil stress due to vertical and horizontal surface forces [3].

3.1.2 Vertical soil stress distribution due to lateral surface forces (Cerruti model)

Moving vehicles add complexity to a vehicle-terrain interaction model. To produce mobility, longitudinal forces (horizontal in the opposite direction of travel) must be supported by the soil. These forces produce wheel or track slip and produce additional soil deformation. The ability of the soil to support wheel/track tractive forces can best be described by both the soil shear strength parameters (cohesion and angle of internal friction) and the soil shear deformation modulus (describes the shear stress/deformation relationship of the soil).

Both longitudinal and lateral horizontal shear forces are known to produce vertical subsurface stresses. These vertical stresses result in increased vehicle sinkage. The phenomenon of slip (longitudinal forces) increasing sinkage is known as slip-sinkage. In-field tests of turning vehicles and laboratory tests have shown that lateral stresses produce lateral displacement and increased sinkage. This additional sinkage is considered “slide sinkage.”

The method for calculating the vertical stress in a semi-infinite, homogeneous, isotropic, elastic medium subject to a horizontal point load applied on the surface was first developed by Cerruti as shown in Eq. (2):

$$\sigma_z = \frac{3}{2\pi} \frac{r(\cos \Theta)}{[1 + (r/z)^2]^{5/2}} \frac{H}{z^3} \quad (2)$$

Where σ_z is the vertical stress at the depth z , H is the horizontal force (lateral or longitudinal), Θ is the angle between the applied force direction and the direction to the location of the vertical stress, and r is the horizontal distance from the point load to the location of the vertical stress (Fig. 1) [3]. These horizontal loads induced vertical stresses are added to the vertical stresses produced from the tire/track vertical soil surface forces, to produce the total vertical stress at a subsurface point.

3.1.3 Vertical soil deformation (sinkage) due to surface forces

After the subsurface vertical stress distribution is determined, soil strain (or compaction) is based on soil visco-elasto-plastic relationships. These relationships are defined for the terrain codes described in the Ethan Allan Firing Rang (EAFR) terrain database. Richmond (2006) indicates that the terrain's Unified Soil Classification System (USCS) soil type, Rating Cone Index (*RCI*), and moisture condition are provided for each terrain code [4]. The constitutive (stress/strain) relationships for each EAFR terrain code must be defined to characterize the soil response (sinkage) due to loading.

The linear portion of the Virgin Compression Curve (VCC) in Fig. 2 can be described for a given water content, or degree of water saturation, S_k , while curves for other water contents can be computed from the following relationship [5]:

$$\rho = [\rho_k + S_T(S_1 - S_k)] + C \log_{10}(\sigma_a / \sigma_k) \quad (3)$$

Where ρ is the computed bulk density, ρ_k is the density at a known stress, S_T is the slope of the bulk density vs. degree of water saturation curve at a given stress, S_1 is the desired degree of saturation, C is the slope of the line shown in Fig. 2, σ_a is the applied normal stress, and σ_k is the known normal stress associated with the known bulk density (ρ_k). σ_a / σ_k is the log stress ratio, and the horizontal axis in Fig. 2 represents this ratio. If the VCC represents a dry soil, lines for soils at water contents less than the given degree of saturation are shifted to the left and parallel the given VCC [5].

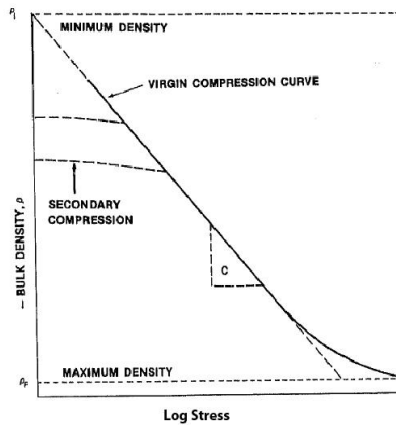


Fig. 2. Theoretical bulk density-stress curve [5].

3.1.4 Rebound constant

The time-dependent elastic and plastic properties EAFR terrain code are needed to fully describe the soil's response to tire/track loads. The rebound properties of a soil are defined by the soil rebound constant (g/cm^3) which defines the bulk density decrease or increase in the soil volume that occurs during/after the soil surface is subject to the loading and unloading of an applied normal load. This can be seen in Fig. 3.

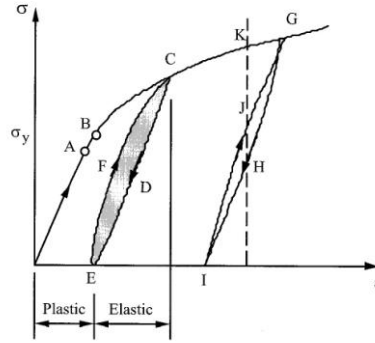


Fig. 3. Soil response to loading and unloading of an applied normal load [6].

3.2 Longitudinal and lateral force calculations

3.2.1 Soil deformation due to shear forces (slip and turning)

Turning vehicles add even more complexity to the vehicle-terrain interaction model. For wheeled vehicles, the forces include the static weight, plus any dynamic weight (due to weight transfer), plus increased longitudinal forces (vehicle rolling resistance increases with turning) producing wheel slip, plus centrifugal (lateral) forces due to the turning radius and velocity, along with any forces produced as non-turning wheels or tracks are dragged across the soil surface.

The ability of the soil to support wheel/track tractive and turning forces can be described by both the soil shear strength parameters (cohesion and friction angle), the soil shear deformation modulus (describes the shear stress/deformation relationship of the soil), and lateral bulldozing forces. The lateral movement of the wheels of a turning vehicle, and the slip occurring in the longitudinal direction will produce shear stress, and cause shear displacement of the soil. A study of the relationship between the shear stress and shear displacement of soils helps understand both the terrain deformation and the required energy and power. Wong [2] indicated that there are three types of relationships between shear stress and shear displacement. The shear stress-shear displacement curves of terrains composed of loose sand or saturated clay along with the majority of disturbed soils can be predicted from an exponential function where the shear stress approaches a theoretical asymptotic shear stress value [2]. A physics-based shear stress-displacement model was proposed by Janosi and Hanamoto and is represented by the following:

$$\tau = \tau_{\max} \cdot \left(1 - e^{-j/K}\right) = (c + \sigma \cdot \tan(\varphi)) \cdot \left(1 - e^{-j/K}\right) \quad (4)$$

Where τ is the shear stress, τ_{\max} is the maximum possible shear stress at the given normal stress (σ), j is the shear displacement, K is the shear deformation modulus, c is the internal cohesion of the soil, and φ is the angle of internal friction of the soil [2].

For turning wheeled vehicles, the lateral shear stress resulting from the centrifugal force produces an applied shear displacement. The shear force (stress multiplied by contact area) multiplied by the shear displacement results in the shearing energy for the turning vehicle. For a turning tracked

vehicle, the track slides back and forth a significant amount. This track slide produces lateral soil displacement. Equation (4) can then be applied to determine the resulting lateral forces.

3.2.2 Lateral and longitudinal forces due to bulldozing

In addition to the shear displacement resulting at the tire/track and soil interface, any tire/track sinkage will create a bulldozing effect that pushes the soil to form outside piles on both sides of the tire/track. The force to push soil is dependent on the tire sinkage/rut depth and the soil strength parameters (c and ϕ).

When soil is pushed by the tire or track, the force required to shear and displace soil can be substantial. The force required to bulldoze the soil can be modeled using the Passive Lateral Earth Pressure theory. The forces resisting bulldozing are the weight of the soil and the shear forces along a defined failure plane. To simplify calculations, negligible friction between the soil and the tire/track face can be assumed which results in a straight failure plane between the bottom of the tire/track and the soil surface. The angle of failure plane is $(\pi/4 - \phi/2)$.

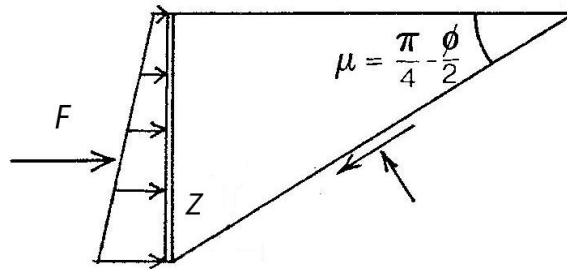


Fig. 4. A representation of the forces/deformation relationship on a turning wheel or track due to bulldozing [7].

The total force at failure of a sunken tire/track shearing and displacing a soil wedge is defined as

$$F = b(\frac{1}{2} \gamma Z^2 N_\phi + 2cZ \sqrt{N_\phi}) \quad (5)$$

Where F is the bulldozing force at failure, b is the width of the element, γ is the soil unit weight, Z is the height of the bulldozed soil wedge, and

$$N_\phi = \tan^2(45 + \phi/2) \quad (6)$$

To determine the bulldozing force at soil failure, the soil strength parameters, soil density, sinkage and width of the contact area are needed. If the bulldozing lateral displacement is known, then the required bulldozing force is reduced by the amount $(1 - e^{-j/K})$, where j is the shear displacement and K is the shear deformation modulus. It should be noted that as the tire/track sinks, Z increases and the

bulldozing force also increases for a given displacement. If the net lateral force required for a vehicle during turning is known, then the lateral displacement can be estimated.

4. Results and discussion

4.1 Vertical soil deformation

4.1.1 Effect of vehicle travel speed

The results from the soils model are presented for the U.S. Army's Stryker Infantry Carrier Vehicle (ICV) traversing a Unified Soils Classification System (USCS) CL soil type. The Stryker is an 8-wheeled, 17,237 kg vehicle that is powered by a 261 kW V-8 diesel engine. The maximum travel speed of the vehicle is 27 m/s. All wheels are equipped with Michelin X tires. The critical Stryker vehicle and tire parameters required as inputs into the physics-based soil model are shown in Table 1. An equal normal load on each tire and negligible weight transfer was assumed. The soil engineering properties estimated for a CL Ethan Allan Firing Range (EAFR) terrain code were used to generate the results from the model, and the properties can be found in the Table 2. The soil deformation time constant was assigned a value of 0.2 s, and this time constant value was an indicator of the time required for the soil's bulk density to increase due to an applied stress, and decrease after unloading of the applied stress by the magnitude of the rebound constant value.

Table 1. Pertinent Stryker vehicle and tire parameters.

Stryker Vehicle/Tire Parameters	
Vehicle weight (kN):	169
Tire diameter (m):	1.118
Tire section width (m):	0.279
Tire section height (m)	0.552

Table 2. The required input soil parameters to the model.

Soil Properties	
USCS Soil Type:	CL
Moisture Condition:	Slippery
RCI_{AVG} (kPa)	552
ρ (g/cm^3):	1.25
S_1 (%):	50
c (kPa):	27.4
ϕ ($^\circ$):	17
K (m):	0.10
Rebound constant (g/cm^3)	0.02
Deformation time constant (s)	0.2

MATLAB code was used to develop the initial output from the model according to the equations provided in Section 3. For demonstration purposes, the change in bulk density and the power dissipated due to the vertical deformation of a single soil element with a volume of 1 cm^3 was calculated. The soil element was assumed to be 5 cm below a horizontal soil surface along the centerline of four Stryker tires. The vertical stress exerted on the soil element from the Stryker tires was estimated via Eq. (1) while assuming the normal load on each tire was equal. The change in bulk

density of the soil element that was subject to the repetitive applied vertical stress due to the normal loads from the tires from a Stryker vehicle traveling at 3.0 m/s is given in Fig. 5 as a function of time. The power dissipated due to the deformation of the soil element is represented in Fig. 6.

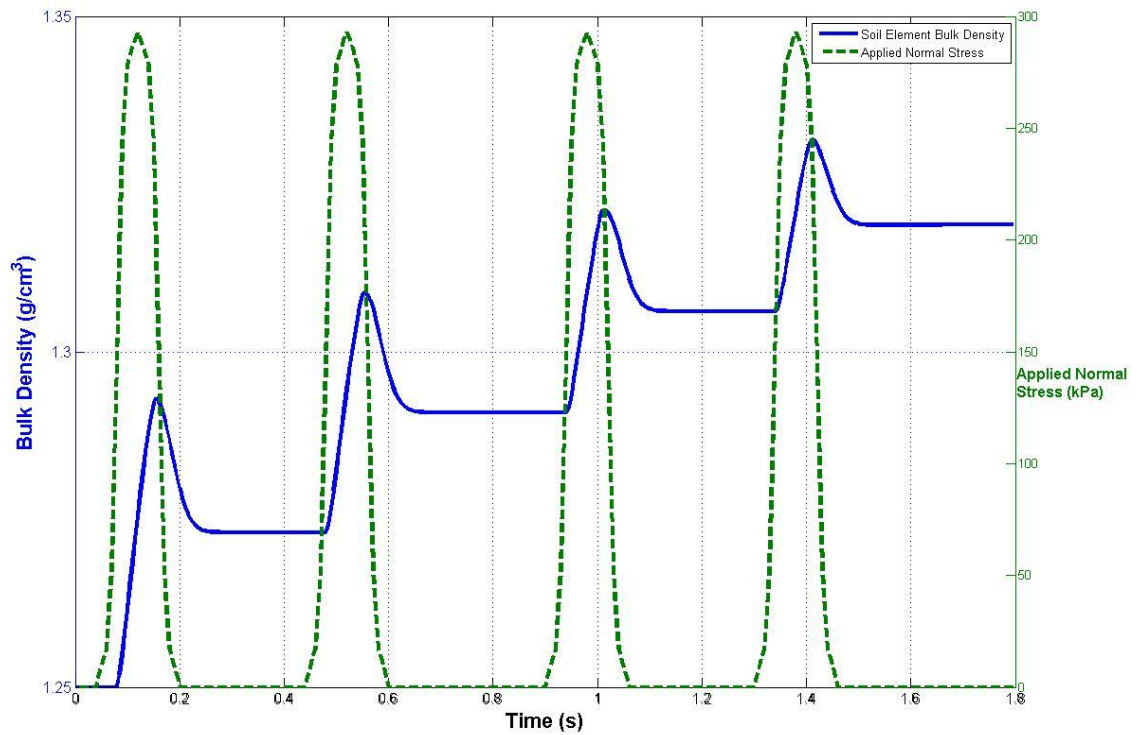


Fig. 5. The bulk density change of a single soil element due to a Stryker vehicle traveling at 3.0 m/s.

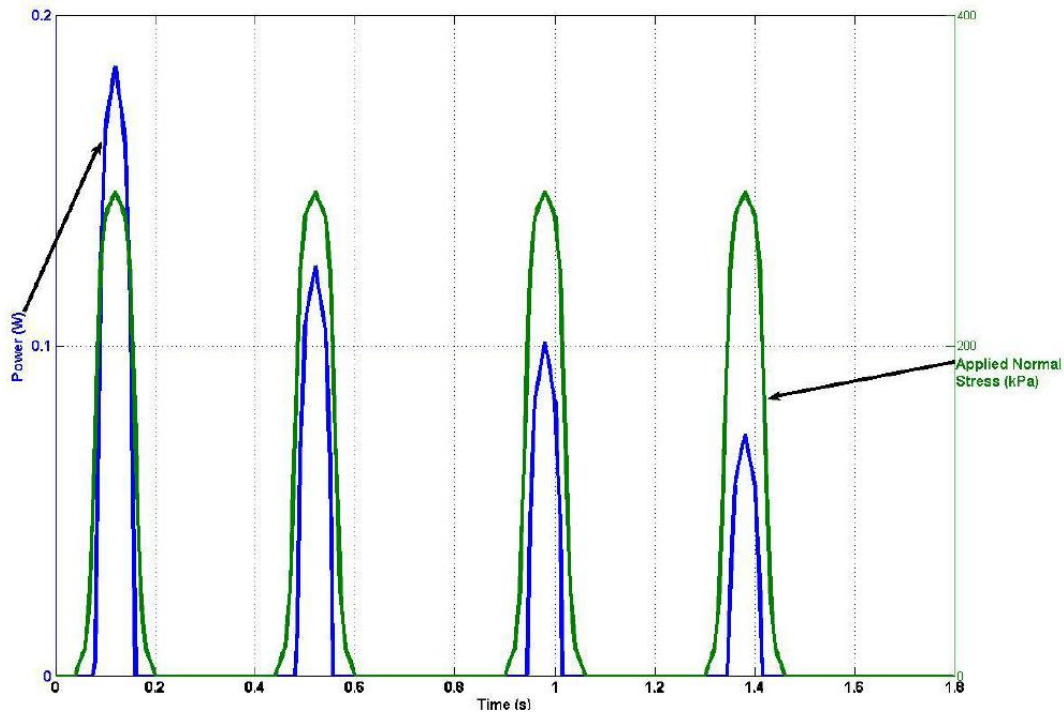


Fig. 6. The power dissipated due to the deformation of a single soil element due to a Stryker vehicle traveling at 3.0 m/s.

The increase in bulk density of the soil element and the subsequent power required decreased as the number of passes by the tires of the Stryker vehicle increased. The power dissipated from the tires to the soil element decreased because of the reduced initial sinkage, resulting from the increase in the soil element's bulk density. The bulk density increased by an average of 14% after each pass of the Stryker vehicle's four tires. The maximum power value during each pass decreased by an average of 27%. The change in bulk density of the soil element subject to the repetitive applied vertical stress of the tires from a Stryker vehicle traveling at 1.5, 3.0, and 6.0 m/s is provided in Fig. 7.

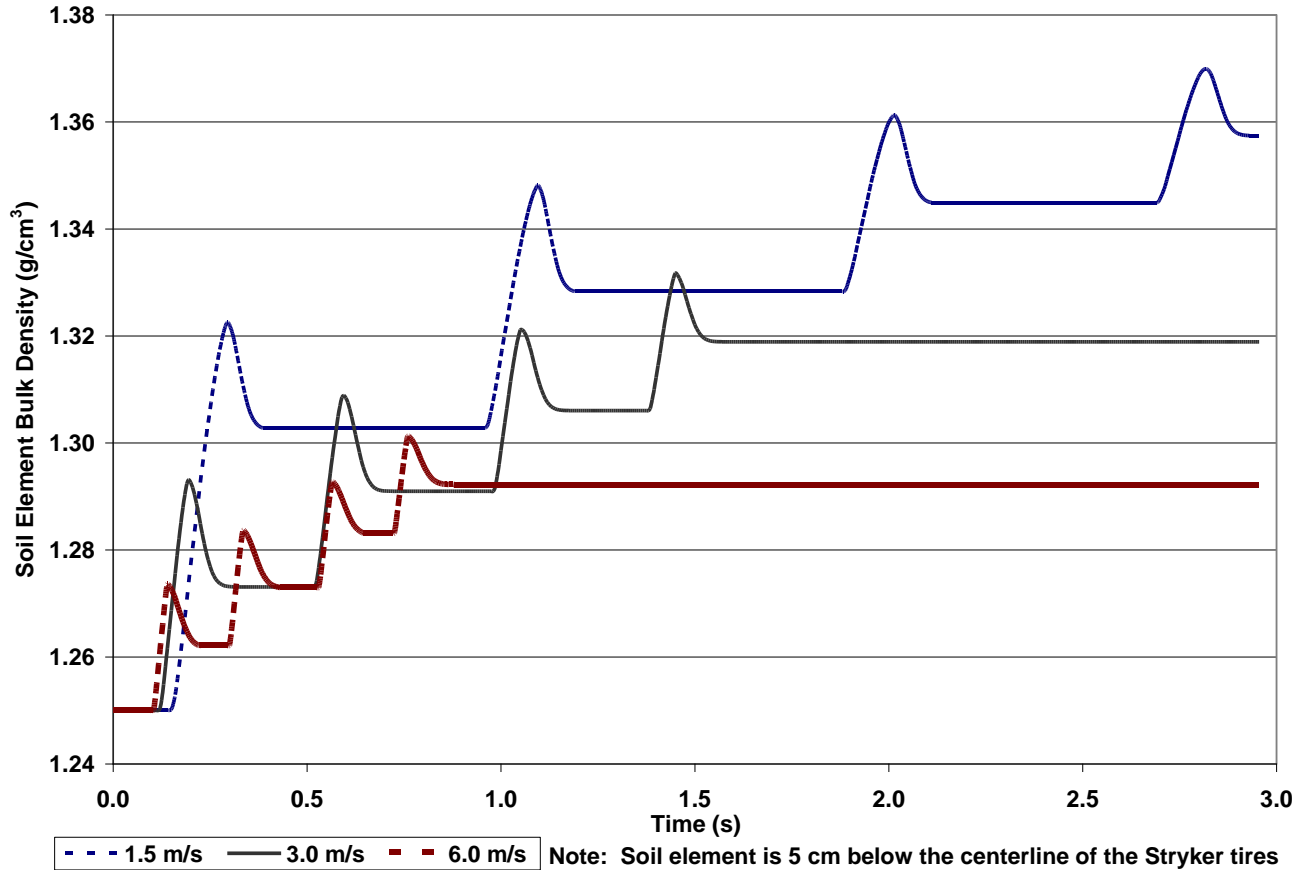


Fig. 7. The change in bulk density of a single soil element due to a Stryker vehicle at three levels of travel speed.

The soil element's increase in bulk density decreased as the Stryker vehicle's travel speed increased which indicated that the net energy transferred to the soil element due the deformation of the element also decreased as travel speed increased. As the vehicle travel speed increased from 1.5 m/s to 3.0 and 6.0 m/s, the soil element's final increase in bulk density decreased by 2.9 and 4.8% respectively.

4.1.2 Effect of soil moisture content

The effect of varying the soil element's degree of saturation (S_k) had on the subsequent deformation of the element is represented in Fig. 8.

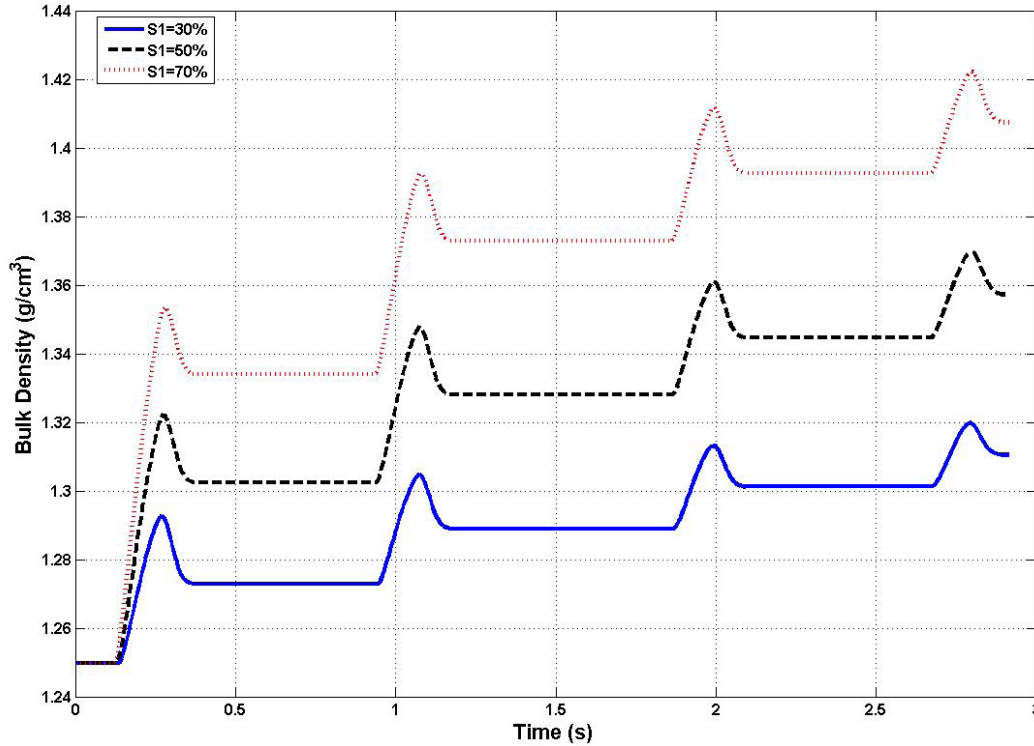


Fig. 8. The change in bulk density of a single soil element at three levels of soil degree of saturation at a travel speed of 1.5 m/s.

The bulk density increase of the soil element due to the vertical stress from the Stryker tires increased as the degree of saturation (S_k) of the soil element increased. As S_k increased from 30% to 50% and 70%, the final bulk density of the soil element increased by approximately 3.6 and 7.4%, respectively.

4.2 Lateral soil bulldozing

The estimated lateral displacement and power as a function of turning radius and travel speed for a single Stryker tire are shown in the Fig. 9 and 10 at travel speeds of 1.5, 3.0, and 6.0 m/s. The tire sinkage was assumed to be a constant 0.05 m for the for the model output shown in Fig. 9 and 10.

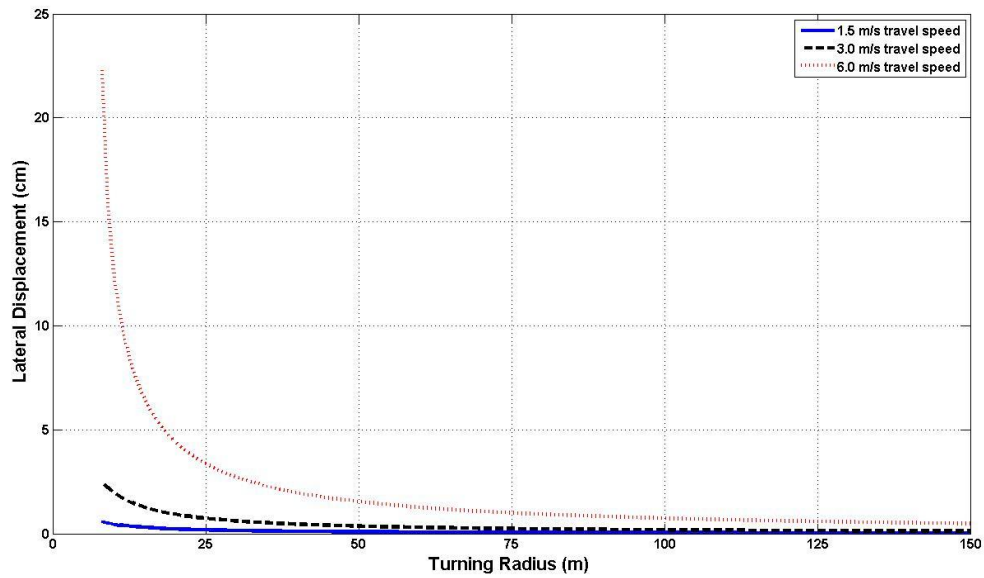


Fig. 9. The average lateral displacement of the CL USCS soil type as a function turning radius at a constant tire sinkage of 0.05 m and three levels of Stryker travel speed.

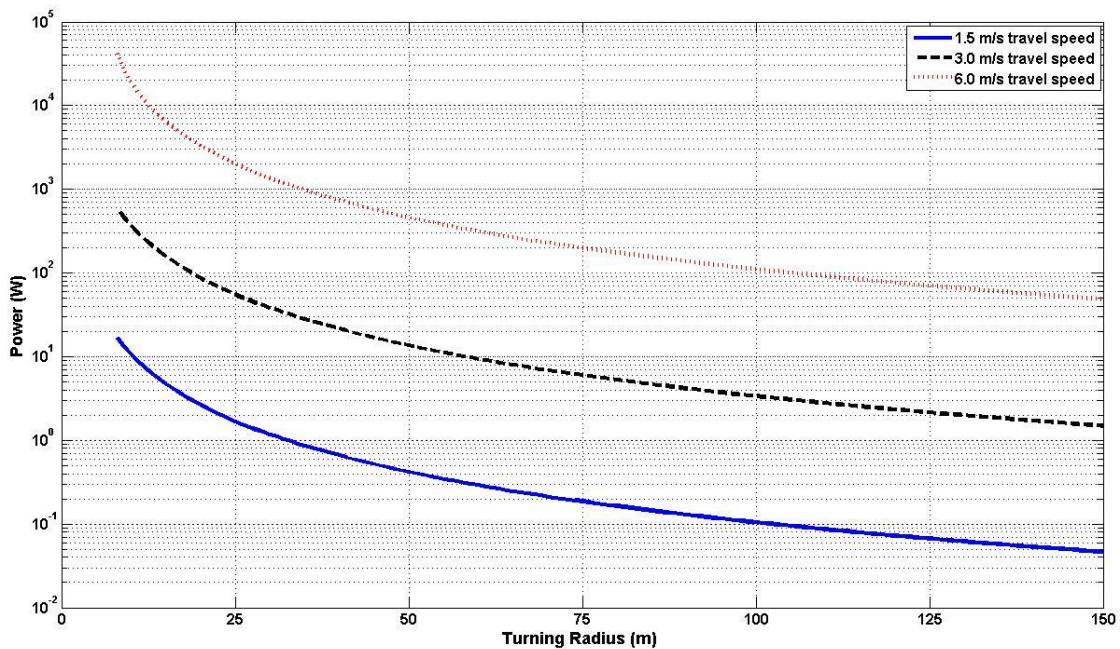


Fig. 10. The power required at a given turning radius for a Stryker vehicle traveling with a constant tire sinkage of 0.05 m at three levels of travel speed.

The lateral displacement and power required increased as the Stryker vehicle's travel speed increased and the vehicle's turning radius decreased. The power requirement of the Stryker vehicle traveling at a tire sinkage of 0.05 m increased by 1.5 orders of magnitude as the travel speed increased from 1.5 m/s to 3.0 and 6.0 m/s. The average lateral displacement of the CL USCS soil type as a function of tire sinkage (ie rut depth) for a Stryker vehicle traveling at 3.0 m/s while maintaining a turning radius

of 30 m is given in Fig. 11. The maximum theoretical travel speed of the Stryker vehicle as a function of turning radius before it would theoretically begin to slide-out is represented in Fig. 12 at a constant tire sinkage of 0.05 m.

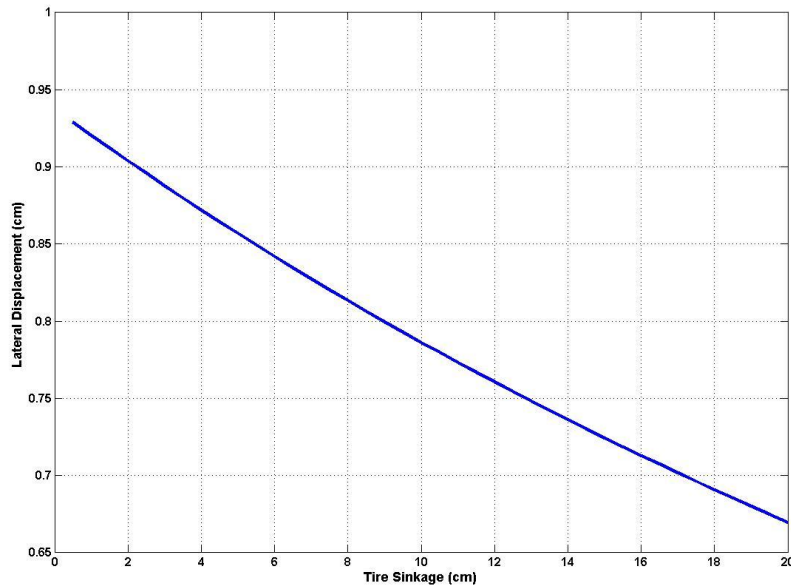


Fig. 11. The average lateral displacement of the CL soil type as a function of the Stryker tire's sinkage at a travel speed and turning radius of 3.0 m/s and 30 m.

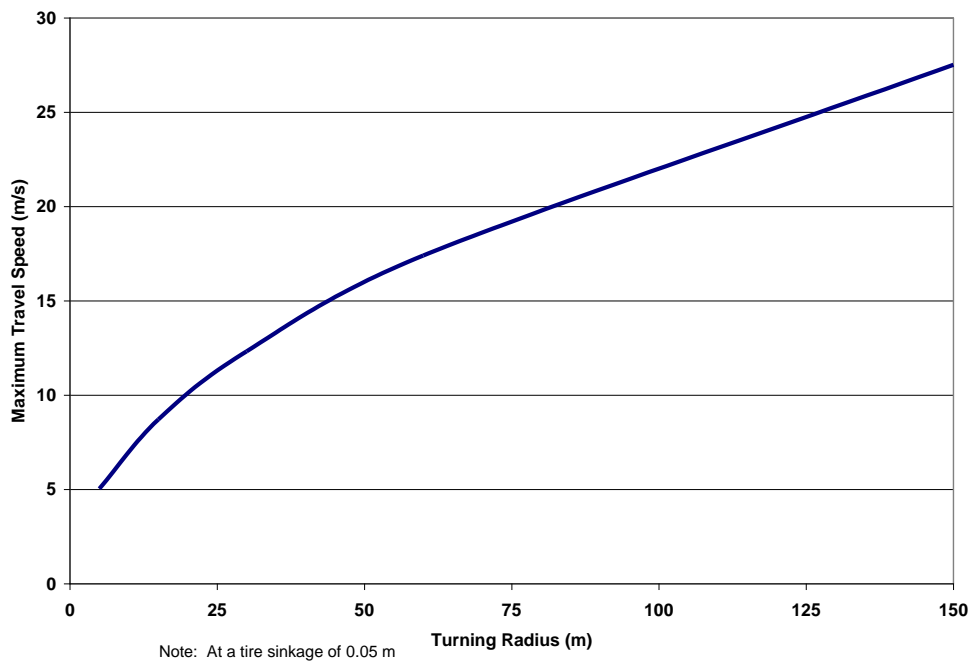


Fig. 12. The theoretical maximum travel speed of the Stryker vehicle at a tire sinkage of 0.05 m while operating on a CL USCS soil type.

The average lateral displacement and power both tended to increase substantially when the turning radius of the Stryker was less than 25 m at a tire sinkage of 0.05 m. The maximum travel speed at a tire sinkage of 0.05 m increased as the vehicle turning radius increased. The Stryker vehicle would theoretically not be able to exceed the travel speed shown in Fig. 12 at the given turning radius and tire sinkage because it would be exceeding the soil's maximum shear strength. The soil's shear strength provides the inward lateral force required for the Stryker vehicle to perform a turn at the given travel speed, turning radius, and tire sinkage.

4.3 Longitudinal soil bulldozing

Fig. 13 below represents the longitudinal bulldozing power requirement for a single Stryker tire as a function of rut depth while operating on the EAFR terrain code detailed in the Table 2. The height of the soil wedge displaced during longitudinal bulldozing is a function of the angle of the failure plane ($\pi/4 - \phi/2$). It is assumed that only the soil above the failure plane that tangentially intersects the edge of the tire is longitudinally bulldozed (ie some fraction of the rut depth).

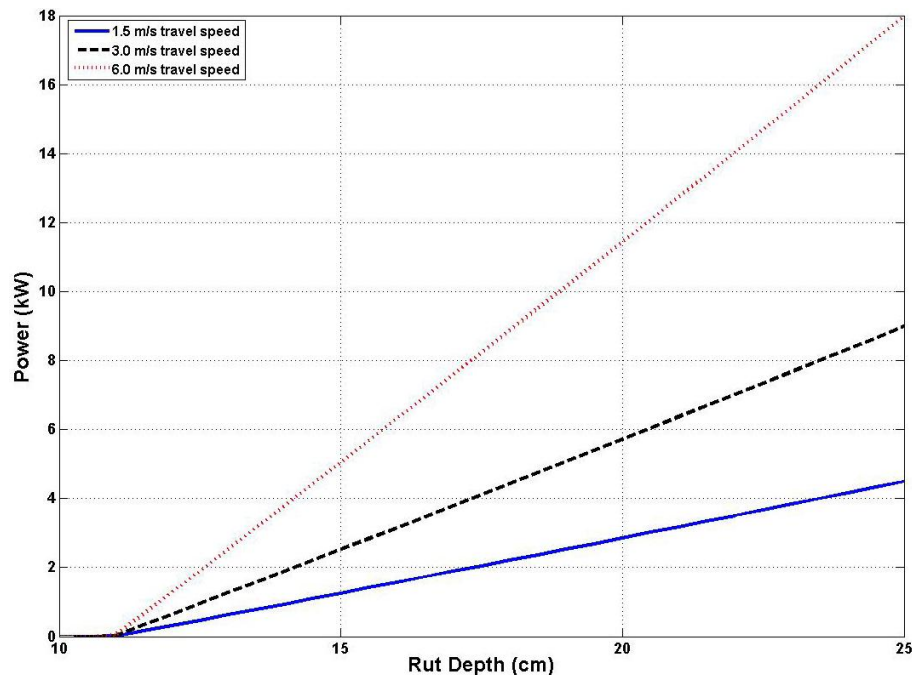


Fig. 13. The power dissipated due to the longitudinal bulldozing of a CL soil type as a function of the Stryker tire's rut depth (ie tire sinkage) at three levels of travel speed.

The power required to overcome longitudinal bulldozing does not occur until a tire sinkage of approximately 11.5 cm is attained because of the theory governing the model, the engineering soil properties, and the geometry of the tire. The longitudinal bulldozing power requirement while operating at a travel speed of 6.0 m/s was approximately 50 and 76% greater than the power required at a travel speed of 3.0 and 1.5 m/s respectively. A sensitivity analysis was done using the vehicle and terrain parameters given in Tables 1 and 2 respectively to determine the effect of varying the angle of internal friction (ϕ) on the required longitudinal bulldozing power for a single Stryker tire (Note: cohesion (c) remained a constant 27.4 kPa), and the results are summarized in Fig. 14.

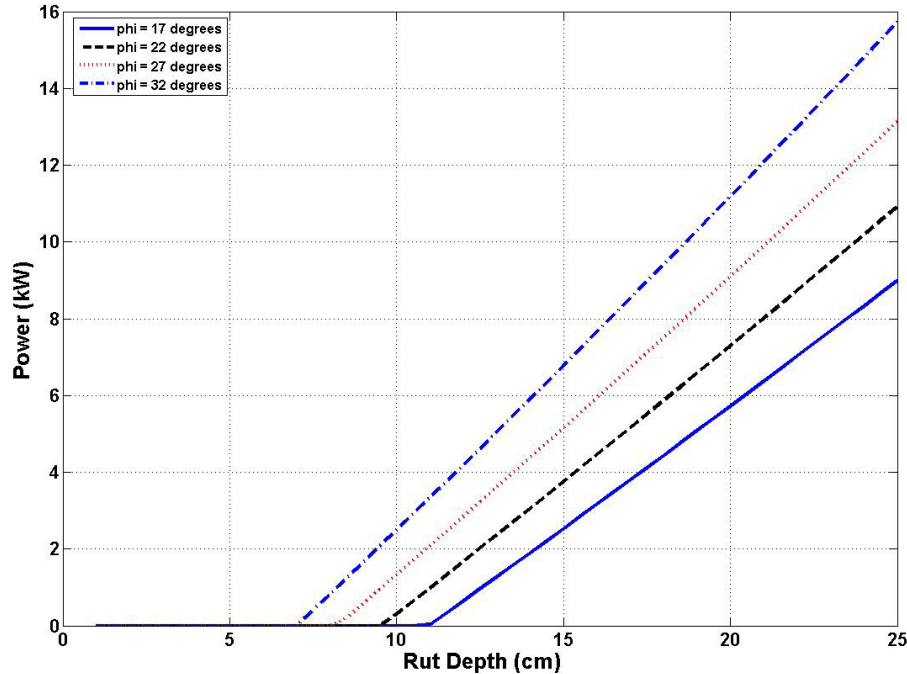


Fig. 14. The effect of varying the CL USCS soil type's angle of internal friction has on the power dissipated by a single Stryker tire due to longitudinal bulldozing.

The predicted power required to overcome the longitudinal bulldozing force generated by a single Stryker tire increased as the angle of internal friction increased. The power increased as the angle of internal friction (ϕ) increased because the angle of the failure plane ($\pi/4 - \phi/2$) decreased, resulting in a soil wedge with a greater volume displaced while the shear strength increased along the failure plane.

5. Conclusions

A physics-based, deformable soil model can be used to characterize the response of an off-road terrain due to a military vehicle. The governing equations require that the soil engineering properties be defined for the given terrain. Initial results from the physics-based model were presented for a single soil element (Unified Soils Classification System (USCS) CL soil type) 5 cm below the soil surface subject to repetitive loading from four of the Stryker vehicle's tires. The model provided for reasonable estimates of the soil elements variation in bulk density and the associated power dissipated by the tires to the soil element. The power exerted on the soil element by the tires decreased as the number of passes by the tires increased, and the bulk density increase due to the pass of each tire decreased as the number passes increased. The increase in bulk density increased as the degree of saturation of the soil element increased.

The average lateral displacement of the soil and the power requirement while the Stryker vehicle was turning was characterized. The average lateral displacement from all eight of the Stryker vehicle's tires and the associated power requirement tended to increase as the travel speed increased and the vehicle turning radius decreased. The maximum travel speed at a tire sinkage of 0.05 m increased as the vehicle turning radius increased. The longitudinal bulldozing component of the model indicated that the power required to overcome the longitudinal bulldozing from a single Stryker tire increased as the tire sinkage (rut depth), vehicle travel speed, and the soil's angle of internal friction increased.

Preliminary application of the physics-based, deformable soil model demonstrated that the model provided reasonable estimates of the power dissipated to a single soil element and the power required for a turning vehicle operating in an off-road environment.

6. Recommendations

Full-scale implementation of the soils model into a real-time, physics-based Vehicle-Terrain Interaction (VTI) model must be done in order to fully assess the validity of the soils model. Madsen (2012) details the initial efforts to implement the physics-based soil model into a complete physics-based VTI model [1]. Furthermore, in-field validation of the soil model is necessary in order to determine the accuracy of the model. Future validation of the model will occur by operating a military vehicle in an off-road environment. The model's predicted soil response, power, and energy requirements will be compared to the measured values.

Nomenclature

σ	Vertical stress	[kPa]
z	Depth below soil surface	[m]
W	Vertical point load	[kN]
r	Horizontal distance from point load	[m]
H	Horizontal force load	[kN]
Θ	Angle between point load and stress vectors	[°]
RCI	Rating cone index	[kPa]
ρ	Dry bulk density	[g/cm ³]
S	Degree of saturation	[%]
C	Compression index	[g/cm ³]
τ	Shear Stress	[kPa]
j	Shear displacement	[m]
K	Shear deformation modulus	[m]
c	Cohesion	[kPa]
φ	Angle of internal friction	[°]
F	Bulldozing force generated at soil failure	[kN]
Z	Height of the bulldozed soil wedge	[m]

References

- [1] Madsen J, Negrut D, Reid A, Seidl A, Ayers P, Bozdech G, Freeman J, O'Kins J. A physics-based vehicle/terrain interaction model for soft soil off-road vehicle simulations. SAE Paper No. 2012-01-0767. 2012.
- [2] Wong JY. Theory of ground vehicles. 4th ed. NJ: Wiley; 2008.
- [3] Fedá J. Stress in subsoil and methods of final settlement calculation. NY: Maxwell; 1978.
- [4] Richmond PW, Shoop SA, Reid AA, Mason GL. Terrain surface codes for an all-season, off-road ride motion simulator. In: MSIAC M&S Journal On-line, <http://www.msiac.dmsi.mil/journal>; 2006.
- [5] Larson WE, Gupta SC, Useche RA. Compression of agricultural soils from eight soil orders. Soil Sci Soc Am J 1980; 44:450–457.
- [6] Upadhyaya SK et al. Advances in soil dynamics. Vol 2. St. Joseph, MI: ASAE; 2002.
- [7] Holtz RD, Kovacs WD. An Introduction to geotechnical engineering. NJ: Prentice-Hall, Inc; 1981.